

**PRELIMINARY IRON DISTRIBUTION ON VESTA.** N. Yamashita<sup>1</sup>, T.H. Prettyman<sup>1</sup>, R.C. Reedy<sup>1</sup>, W.C. Feldman<sup>1</sup>, D.J. Lawrence<sup>2</sup>, P.N. Peplowski<sup>2</sup>, D.W. Mittlefehldt<sup>3</sup>, H.Y. McSween<sup>4</sup>, T.J. McCoy<sup>5</sup>, M.J. Toplis<sup>6</sup>, O. Forni<sup>6</sup>, H. Mizzon<sup>6</sup>, and C.T. Russell<sup>7</sup>, <sup>1</sup>Planetary Science Institute (1700 East Fort Lowell, Suite 106, Tucson, AZ 85719-2395, yamashita@psi.edu), <sup>2</sup>Johns Hopkins University Applied Physics Laboratory, <sup>3</sup>NASA Johnson Space Center, <sup>4</sup>Earth & Planetary Sciences, University of Tennessee, Knoxville, TN 37996, <sup>5</sup>Smithsonian Institution, <sup>6</sup>University of Toulouse, France, <sup>7</sup>University of California, Los Angeles.

**Introduction:** The distribution of iron on the surface of the asteroid Vesta was investigated using Dawn's Gamma Ray and Neutron Detector (GRaND) [1,2]. Iron varies predictably with rock type for the howardite, eucrite, and diogenite (HED) meteorites, thought to be representative of Vesta. The abundance of Fe in howardites ranges from about 12 to 15 wt.%. Basaltic eucrites have the highest abundance, whereas, lower crustal and upper mantle materials (cumulate eucrites and diogenites) have the lowest, and howardites are intermediate [3].

We have completed a mapping study of 7.6 MeV gamma rays produced by neutron capture by Fe as measured by the bismuth germanate (BGO) detector of GRaND [1]. The procedures to determine Fe counting rates are presented in detail here, along with a preliminary distribution map, constituting the necessary initial step to quantification of Fe abundances.

We find that the global distribution of Fe counting rates is generally consistent with independent mineralogical and compositional inferences obtained by other instruments on Dawn such as measurements of pyroxene absorption bands by the Visual and Infrared Spectrometer (VIR) [4] and Framing Camera (FC) [5] and neutron absorption measurements by GRaND [6].

**Observations:** The BGO detector measures gamma rays emitted from the surface with energies from 0.3 MeV to 9 MeV. Energies of characteristic gamma rays are unique to the source nuclide from which the gamma rays are emitted, and their intensities are proportional to the abundance of the source nuclide after appropriate corrections [7]. In this work, the neutron-capture gamma rays from <sup>56</sup>Fe at 7.6 MeV, which appear as a distinct peak in the BGO pulse height spectrum, were used to study the surface distribution of Fe on Vesta. The observation was sensitive to depths of a few tens of cm.

The gamma-ray data for mapping were acquired during the low altitude mapping orbit (LAMO), which took place from December 2011 to May 2012. The average altitude was 210 km. To determine the background contribution, data acquired during the Vesta Survey period, which took place at more than 2700 km away from Vesta's surface, were analyzed. Science data acquired during both LAMO and Survey are available from NASA's Planetary Data System.

**Spectral analysis:** The net counting rate of the Fe gamma ray peak was determined for all the time-ordered records by subtracting background counts from the gross counts within the 7.6 MeV peak region of interest (ROI). The ROI was determined based on peak centroid energies of Fe and surrounding gamma ray peaks. The background for the Fe peak was determined using the higher energy portion of the spectrum where no peaks exist and fitted to an exponential curve (an example is shown in Fig. 1). After the background subtraction, the net counts were corrected for live times, the solid angle subtended by Vesta at the spacecraft, and intensities of galactic cosmic rays using the counting rate for coincidences with three or more sensors of GRaND [1]. The average counting rate was ~0.074 counts/s. The Survey spectrum in Fig. 1, which was scaled for comparison with the LAMO spectrum, shows that the 7.6-MeV signature is of vestan origin.

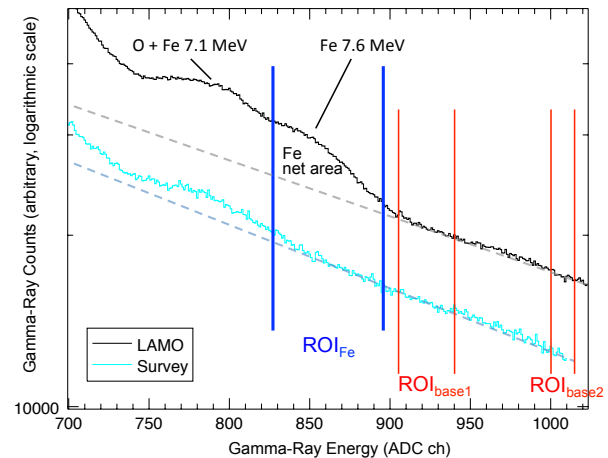


Fig. 1. Energy spectra of gamma rays from 6.2 MeV to 9.1 MeV obtained by the BGO detector in GRaND during LAMO and Survey. The baselines for the Fe peak fitted at  $ROI_{base1}$  and  $ROI_{base2}$  with exponential curves are shown by the dashed lines to derive the net counts.

*Correction for neutron number density and hydrogen content.* Since the Fe gamma rays measured by GRaND are produced by neutron capture reactions, the Fe counting rate is proportional to the abundance of Fe and the number density of neutrons in the regolith [8].

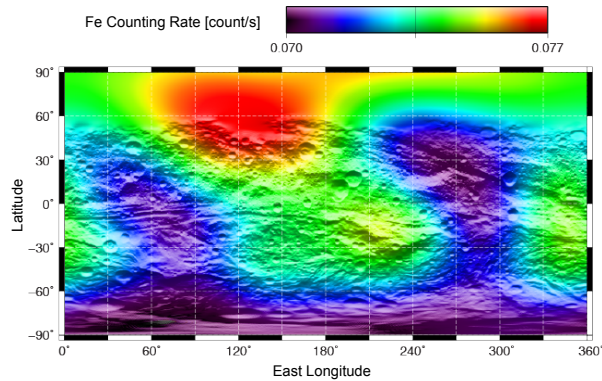


Fig. 2. Global distribution of Fe counting rates on the surface of Vesta measured by the BGO detector of GRaND, with a boxcar smoothing with a radius of  $30^\circ$ . Note that this map is not corrected for variations of neutrons at the subsurface and therefore considered as preliminary.

Thus, Fe abundance is not strictly proportional to Fe counting rate, as was demonstrated by Lunar Prospector [9]. At Vesta, neutron number density variations are caused by major elements as well as by hydrogen [3]. Full corrections are still under development [1,3,6,10]. Consequently, Fe counting rates as a proxy for the variation of the abundance of Fe are presented in this abstract.

**Preliminary Results:** The net counting rate of the Fe gamma-ray peak was mapped globally, as shown in

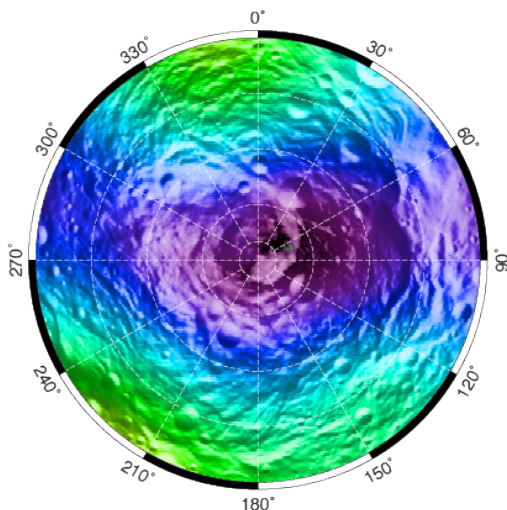


Fig. 3 Distribution of Fe counting rates in the southern hemisphere from  $-30^\circ$  to  $-90^\circ$  in latitude with stereographic projection. The same color bar and smoothing technique were used as those in Fig. 2. Note that this map is not corrected for variations of neutrons at the subsurface and therefore considered as preliminary.

Fig. 2. The map exhibits the highest Fe counting rate in the northern hemisphere. The hydrogen-rich regions discovered by neutron observations near the equator [3] have in general intermediate counting rates. The Fe counting rate is lowest in the Rheasilvia basin at the south pole region and extends as two lobes across the equator; one to the west at  $\sim 75^\circ$  longitude and the other at  $\sim 285^\circ$  in the east near a basin containing Oppia. The two-direction, V-shaped distribution near the south pole is more clearly seen in Fig. 3.

Even though these Fe maps have not been fully corrected for variations of neutron number density, Figures 2 and 3 indicate non-uniformity of the elemental Fe abundance in the regolith of Vesta that is correlated with geographical features. Since Fe has the highest macroscopic absorption cross section of neutrons and atomic mass among the major elements, such surface variability has been also confirmed by high- and low-energy neutrons [6,10] as well as high energy gamma rays [11] that are also measured by GRaND. Indeed, the lowest counting rate at the south pole region coincides with the lower counts of fast neutrons and higher counts of thermal plus epithermal neutrons, which can be interpreted as diagenetic materials from lower crust or upper mantle exposed by the Rheasilvia impact. The local maxima near the equator are consistent with eucritic materials.

Fe distribution can be used as an indicator of the petrologic evolution on Vesta, and, together with neutron observations, provides independent information to supplement or confirm mineralogical and optical observations. For example, VIR observations pointed to the presence of diogenite in the west, consistent with our findings for Fe, but did not reveal the eastern lobe [4]. With further refinement of GRaND data, a definitive determination of global Fe abundance is expected.

**Acknowledgements:** This work was funded by the NASA Dawn mission.

**References:** [1] Prettyman T. H. et al. (2011) *Space Sci. Rev.*, 163, 371–459. [2] Russell C. T. et al. (2012) *Science* 336, 684. [3] Prettyman T. H. et al. (2012) *Science*, 338, 242. [4] De Sanctis M. C. et al. (2012) *Science* 336, 697–700. [5] Reddy V. et al. (2012) *Science* 336, 700–704. [6] Prettyman T. H. et al. (2013) *LPS XLIV*, this issue. [7] Reedy R. C. (1978) *Proc. Lunar Planet. Sci. Conf.* 9, 2961–2984. [8] Feldman W. C. et al. (2000) *JGR*, 105, 20347–20363. [9] Lawrence D. J. et al. (2002) *JGR*, 107, 5130. [10] Lawrence D. J. et al. (2013) *LPS XLIV*, this issue. [11] Peplowski P. N. et al. (2013) *LPS XLIV*, this issue.